Available online at www.sciencedirect.com

SciVerse ScienceDirect

Ceramics International 38 (2012) 4285–4293

CERAMICS INTERNATIONAL

www.elsevier.com/locate/ceramint

Effects of composition and crystallite size on the accuracy of the Rietveld method in determining lattice parameters of polytypes in multiphase SiC ceramics

Angel Hernández-Jiménez [a], Angel L. Ortiz [a,*], Florentino Sánchez-Bajo [b], Carlos A. Galán [b]

[a] Departamento de Ingeniería Mecánica, Energética y de los Materiales, Universidad de Extremadura, 06006 Badajoz, Spain
[b] Departamento de Física Aplicada, Universidad de Extremadura, 06006 Badajoz, Spain

Received 23 January 2012; accepted 2 February 2012
Available online 11 February 2012

Abstract

The accuracy of the Rietveld method in determining the lattice parameters of polytypes in multiphase SiC ceramics was investigated as a function of the polytype composition and of the polytype crystallite size, using as benchmarks two sets of standard X-ray diffraction (XRD) patterns obtained by computer simulation. It was found that the Rietveld method is remarkably accurate, but also that the measurement of lattice parameters is sensitive to the polytype composition and to the polytype crystallite size. In particular, the accuracy of Rietveld-calculated lattice parameters for a given polytype not only decreases with increasing number of polytypes in the SiC ceramics, but also depends on which other polytypes are present. These two findings are interpreted based on the severity of the corresponding peak overlap phenomenon in the XRD patterns. In addition, the accuracy of the Rietveld analyses also decreases with decreasing crystallite size of the polytypes, which is due to the progressive loss of definition in the location of the peak maxima and to the greater severity of the peak overlap, both resulting from the corresponding peak broadening. This identification of the confidence limits of the Rietveld-calculated lattice parameters for a wide range of microstructural features may have important implications for the future characterization of SiC ceramics by XRD.

Keywords: D. SiC; Rietveld method; X-ray diffraction; Lattice parameters; Polytypes

Introduction

Liquid-phase sintered (LPS) SiC is one of those important non-oxide engineering ceramics with a wide variety of applications in numerous technological industries because it combines the attractive physicochemical properties of SiC with the economy and ease of pressureless liquid-phase processing. Owing to the use of oxide additives (generally combinations of Al_2O_3 with Y_2O_3 or some other rare-earth oxide [1,2]) that melt during sintering, the microstructure of LPS SiC comprises SiC grains embedded in an oxide matrix. In addition, because coarsening in LPS SiC occurs by solution-reprecipitation [3–6], another of its typical microstructural features is that the SiC grains exhibit what is known as a ''core–shell'' structure, where the core is pure SiC and the shell is SiC with trace amounts of atoms picked up from the liquid phase during the reprecipitation stage [3–7]. The ''core–shell'' substructure is, however, rarely observed in highly coarsened microstructures, but this is due simply to the large size of the shell in relation to the core, and also to the occurrence of diffusion-induced chemical homogenization within the SiC grains [4]. Whichever the case, the fact is that the SiC grains in LPS SiC are indeed a complex solid solution rather than pure SiC.

It is well known that there exists a strong correlation between the formation of these solid solutions and the transformations between the SiC polytypes. Thus, whereas the dissolution of group III solutes into SiC creates p-type electronic defects that stabilize the non-cubic α-SiC polytypes (i.e., 2H, 4H, 6H, 15R, etc.) [8], group V solutes create n-type defects that stabilize the cubic β-SiC polytype (i.e., 3C) [8]. This provides the control of the polytype transformations required to tailor the microstructure of LPS SiC from equiaxed grains to elongated grains (commonly referred to as in situ toughened SiC) [4–6,9–11].

* Corresponding author. Tel.: +34 924289600x86726; fax: +34 924289601.
E-mail address: alortiz@materiales.unex.es (A.L. Ortiz).

0272-8842/$36.00
doi:10.1016/j.ceramint.2012.02.009

Some structural and functional properties of LPS SiC have also been found to be affected by the formation of these solution solutions. For example, the hardness increases [12], which has been attributed to the well-documented solid-solution hardening [13]. The mild-wear resistance is expected to increase too because it is dictated by dislocation activity [14]. The electrical conductivity exhibits two temperature-dependence regimes because the core of the SiC grains behaves as an intrinsic semiconductor and the shell as an extrinsic semiconductor [15]. These and other examples indicate that it is necessary to characterize these SiC-based solid solutions to better understand the microstructure and properties of LPS SiC, and a key aspect of the characterization of any solid solution is the accurate determination of its lattice parameters.

In most studies, the measurement of lattice parameters in polycrystalline ceramics is performed by X-ray diffraction (XRD), normally from the experimentally measured peak positions using directly the Bragg law coupled with the plane-spacing equation for the corresponding crystal system [16,17]. However, this simple method cannot be applied to SiC ceramics because they generally comprise a mixture of various polytypes that collectively contribute to the XRD pattern, and the severe peak overlapping induced by their crystallographic similitude would inevitably introduce large errors into the evaluation of the lattice parameters. Thus, in this case the measurement of lattice parameters relies exclusively on the use of the Rietveld method [18,19], which essentially pursues the optimization by non-linear least-squares of a certain model (that includes structural, profile, and instrumental parameters) using the entire diffractogram. While the benefits of using the Rietveld method over other simplified approaches are indisputable, this does not necessarily ensure the measurement of the slight variations in the unit cells of the SiC polytypes with the accuracy required to appropriately investigate these solid solutions as a function of the processing conditions (starting powders, and sintering variables such as atmosphere, time, temperature, additives, etc.). Surprisingly, this fundamental question of whether or not the Rietveld method is indeed able to capture these modifications of the crystal lattice has received little attention, with the exception of an earlier study by some of the present authors devoted to investigating exhaustively the dependence of the accuracy of the lattice parameters measured by the Rietveld method on the geometrical aberrations (zero-angle calibration, off-centering of the sample, and specimen transparency) and the number of polytypes [20]. Clearly, more fundamental studies of this kind are needed prior to using the Rietveld method routinely to determine lattice parameters of polytypes in SiC ceramics. Furthermore, the prime focus of these new works must now be on investigating the dependence of the accuracy of the Rietveld method on microstructural factors, the two most critical of which are doubtless the polytype composition and the crystallite size of the polytypes. A study of the former is vital because SiC ceramics are fabricated from a wide variety of starting powders of the type α, β, or α plus β, and during sintering transformations normally occur between the polytypes. A study of the latter is also important in today's technological context because the combination of new techniques of sintering (i.e., spark-plasma sintering, microwave sintering, or simply two-step sintering with or without pressure) with the commercial availability of nano-powders makes it possible nowadays to fabricate nanostructured, or at least ultrafine-grained SiC ceramics [21]. Furthermore, the SiC grains often contain stacking faults that divide them into different crystallites, which can have sizes in the nanoscale.

With these premises in mind, in the present study we address the aforementioned two issues of the dependence of the accuracy of the lattice parameters measured by the Rietveld method on the polytype composition and on the crystallite size of the polytypes, using to that end two independent sets of standard XRD patterns obtained by computer simulation as benchmarks. Unfortunately, experimental investigation is not possible because there exist no standards of the commonest SiC polytypes with certificated lattice parameters, and the use of the typical commercially available powders would introduce an unnecessary uncertainty into the conclusions. Hence, the use of simulated XRD patterns, of wide-ranging compositions and crystallite sizes as are actual SiC ceramics, was selected as being the best choice for conducting these fundamental studies in a controlled fashion [20]. The details of the simulations, major findings, and analyses will be described below.

Methodological aspects

The two independent sets of 21 standard XRD patterns each which were used in the present study were obtained by computer simulation following the protocol described in detail elsewhere [20]. Consequently, we shall limit ourselves here to summarizing the key steps. Briefly, the individual XRD patterns of the 3C, 4H, 6H, and 15R SiC polytypes were first generated from their crystallographic data, assuming a conventional laboratory diffractometer. Intentionally, the input lattice parameters of the SiC polytypes were enlarged slightly to account for the formation of solid solutions during the liquid-phase sintering. Note that the formation of interstitial solid solutions will enlarge the lattice parameters, as also will the formation of substitutional solid solutions because the ionic radii of C^{4+}, Si^{4+}, Al^{3+}, Y^{3+}, and O^{2-} are 0.15, 0.26, 0.39, 0.9, and 1.21 Å, respectively [22]. Next, these individual patterns were combined in different proportions to reproduce the typical multiphase nature of the SiC ceramics. Subsequently, the instrumental broadening and the geometrical aberrations that are inherent to the experimental collection of XRD data were incorporated, and the resulting XRD patterns were interpolated to emulate a process of data collection in the step-scanning mode. Finally, the background level and the statistical noise, which are present in any experimentally measured XRD pattern, were also introduced. Table 1 gives the general simulation parameters, and Table 2 gives the specific polytype composition and the particular crystallite size of the polytypes chosen for each simulated XRD pattern. As can be observed in Table 2, the effect of the polytype composition was examined using a series of standard XRD patterns prepared with widely ranging combinations of different mixtures of two, three, or

Table 1
Main parameters of the computer simulations chosen to generate the standard XRD patterns used as benchmarks.

Simulation parameters	Description
Diffractometer	Bragg–Brentano geometry with a Cu-tube ($\lambda_{\alpha1}$ = 1.54056 Å, $\lambda_{\alpha2}$ = 1.54439 Å and $I_{\alpha2}/I_{\alpha1}$ = 0.48) and a graphite secondary monochromator
Crystal structures	Distorted 3C (a = 4.3793 Å, α = 90°), 4H (a = 3.0905 Å, c = 10.1048 Å, α = 90°, γ = 120°), 6H (a = 3.0913 Å, c = 15.1398 Å, α = 90°, γ = 120°) and 15R (a = 3.0890 Å, c = 37.8200 Å, α = 90°, γ = 120°)
Crystallite sizes	Variable, in the range of 5–500 nm
Individual patterns	Step-scan mode over a 2θ range of 29–101° with a step width of 0.005°
Phase compositions	Variable, with percentages of polytypes spreading over the range 10–80 wt%
Instrumental broadening	Monte Carlo simulation using the geometrical conditions (goniometer radius, receiving slit, etc.) for a Philips PW-1800 powder diffractometer
Geometrical aberrations	Three: zero-angle calibration (0.02°), off-centering (−0.05°), and transparency (0.02°)
Interpolation	To ensure patterns with constant step of 0.01° over the 2θ range of 30–100°
Background level	Third-order polynomial function (c_0 = 200, c_1 = −2, c_2 = 0.0003, c_3 = 0.0003)
Statistical noise	Poisson distribution

Table 2
Polytype composition and crystallite size of the polytypes in the standard XRD patterns used as benchmarks. Two series of 21 standard XRD patterns each were generated, one to investigate compositional effects and the other to investigate crystallite-size effects.

Standard XRD patterns to study composition effects			Standard XRD patterns to study crystallite-size effects			
No.	Polytypes (weight per cent)	Crystallite sizes (nm) (3C, 4H, 6H, 15R)	No.	Polytypes (weight per cent)	Crystallite sizes (nm)	
					3C	6H
1	20%3C + 80%4H	20	1	50%3C + 50%6H	5	50
2	80%3C + 20%4H	20	2	50%3C + 50%6H	15	50
3	20%3C + 80%6H	20	3	50%3C + 50%6H	30	50
4	80%3C + 20%6H	20	4	50%3C + 50%6H	60	50
5	20%3C + 80%15R	20	5	50%3C + 50%6H	90	50
6	80%3C + 20%15R	20	6	50%3C + 50%6H	200	50
7	20%4H + 80%6H	20	7	50%3C + 50%6H	500	50
8	80%4H + 20%6H	20	8	50%3C + 50%6H	50	5
9	20%4H + 80%15R	20	9	50%3C + 50%6H	50	15
10	80%4H + 20%15R	20	10	50%3C + 50%6H	50	30
11	20%6H + 80%15R	20	11	50%3C + 50%6H	50	60
12	80%6H + 20%15R	20	12	50%3C + 50%6H	50	90
13	50%3C + 50%6H	20	13	50%3C + 50%6H	50	200
14	10%3C + 40%4H + 50%6H	20	14	50%3C + 50%6H	50	500
15	40%3C + 10%4H + 50%15R	20	15	50%3C + 50%6H	5	5
16	50%3C + 40%6H + 10%15R	20	16	50%3C + 50%6H	15	15
17	50%4H + 10%6H + 40%15R	20	17	50%3C + 50%6H	30	30
18	10%3C + 20%4H + 30%6H + 40%15R	20	18	50%3C + 50%6H	60	60
19	40%3C + 10%4H + 20%6H + 30%15R	20	19	50%3C + 50%6H	90	90
20	30%3C + 40%4H + 10%6H + 20%15R	20	20	50%3C + 50%6H	200	200
21	20%3C + 30%4H + 40%6H + 10%15R	20	21	50%3C + 50%6H	500	500

four nanocrystalline polytypes. This was done so as to reproduce the case of SiC ceramics sintered from α, β, or α + β starting powders. The crystallite size of all polytypes in this series was chosen to be 20 nm to induce severe broadening and overlapping of the XRD peaks, which is important in order to be able to extract the secure confidence limits of the Rietveld analyses.

It can also be seen in Table 2 that the effect of the polytype crystallite size was investigated using a series of standard XRD patterns corresponding to the 3C + 6H system model, with variable crystallite size in the range between 5 nm and 0.5 μm for the 3C, 6H, or 3C and 6H polytypes to span different nano-, ultrafine-, and fine-grained microstructures. The choice of the 3C + 6H model system is because it is the two-polytype combination with the greatest degree of peak overlap, which again is important with a view to extracting confidence limits, whereas the choice of 5 nm and of 0.5 μm as lower and upper limits, respectively, for the polytype crystallite size is simply because below 5 nm the polytypes are actually amorphous and because above 0.5 μm the XRD peaks exhibit only instrumental broadening.

The 42 computer-simulated standard XRD patterns were subsequently analyzed using the Rietveld method to determine the lattice parameters of the SiC polytypes present. The Rietveld refinements were implemented using the standard protocol of sequential fit described in detail elsewhere [20,23].

The error of the Rietveld analyses was quantified as the absolute value of the relative difference between the Rietveld-calculated lattice parameters and the lattice parameters used as inputs in the computer simulations. These errors will be taken as empirical estimates of the accuracy of the Rietveld method in determining the lattice parameters of polytypes in multiphase SiC ceramics.

Results and discussion

Influence of the polytype composition

Table 3 gives the lattice parameters of the SiC polytypes calculated by the Rietveld method for the first series of 21 standard XRD patterns, and Table 4 lists the relative error of

Table 3
Lattice parameters of the SiC polytypes determined by the Rietveld method for the first series of 21 simulated standard XRD patterns, designed to investigate compositional effects in the determination of lattice parameters.

No.	Lattice parameters determined from the Rietveld analysis (Å)						
	a_{3C}	a_{4H}	c_{4H}	a_{6H}	c_{6H}	a_{15R}	c_{15R}
1	4.37965(8)	3.09102(4)	10.10596(15)	–	–	–	–
2	4.37980(3)	3.09107(6)	10.10566(26)	–	–	–	–
3	4.38040(8)	–	–	3.09216(4)	15.14417(21)	–	–
4	4.38867(7)	–	–	3.09082(9)	15.13827(52)	–	–
5	4.37928(10)	–	–	–	–	3.08908(6)	37.82101(33)
6	4.37952(4)	–	–	–	–	3.08916(7)	37.82275(104)
7	–	3.09089(6)	10.10565(35)	3.09157(4)	15.14163(27)	–	–
8	–	3.09084(5)	10.10579(17)	3.09140(11)	15.14315(95)	–	–
9	–	3.09099(7)	10.10590(27)	–	–	3.08970(3)	37.82826(46)
10	–	3.09080(2)	10.10581(11)	–	–	3.09067(8)	37.83954(63)
11	–	–	–	3.09141(10)	15.14216(64)	3.08810(11)	37.80965(54)
12	–	–	–	3.09192(3)	15.14168(20)	3.08806(7)	37.81036(72)
13	4.37866(11)	–	–	3.09084(9)	15.13884(52)	–	–
14	4.38031(17)	3.09136(4)	10.10722(21)	3.09204(6)	15.14439(42)	–	–
15	4.38063(11)	3.09146(10)	10.10728(41)	–	–	3.09022(23)	37.83840(93)
16	4.38022(9)	–	–	3.09192(11)	15.14390(37)	3.09021(17)	37.83537(156)
17	–	3.09102(8)	10.10656(21)	3.09187(22)	15.14374(121)	3.09010(16)	37.83315(45)
18	4.38103(17)	3.09203(8)	10.10856(38)	3.09236(9)	15.14763(63)	3.09040(5)	37.83528(76)
19	4.38073(10)	3.09220(14)	10.10705(67)	3.09214(13)	15.14689(86)	3.09027(8)	37.83321(115)
20	4.38074(11)	3.09164(7)	10.10819(28)	3.09174(24)	15.14865(165)	3.09042(10)	37.83109(150)
21	4.38096(9)	3.09184(5)	10.10852(27)	3.09233(7)	15.14694(50)	3.09096(16)	37.83114(209)

Table 4
Absolute value of the relative difference between the lattice parameters of the SiC polytypes calculated by the Rietveld method and those used as inputs in the simulations of the first series of 21 standard XRD patterns, designed to investigate compositional effects in the determination of lattice parameters.

No.	Error of the Rietveld analysis (%)						
	a_{3C}	a_{4H}	c_{4H}	a_{6H}	c_{6H}	a_{15R}	c_{15R}
1	0.00799	0.01683	0.01148	–	–	–	–
2	0.01142	0.01844	0.00851	–	–	–	–
3	0.02512	–	–	0.02782	0.02886	–	–
4	0.01439	–	–	0.01553	0.01011	–	–
5	0.00046	–	–	–	–	0.00259	0.00267
6	0.00502	–	–	–	–	0.00518	0.00727
7	–	0.01262	0.00841	0.00873	0.01209	–	–
8	–	0.01100	0.00980	0.00323	0.02213	–	–
9	–	0.01586	0.01089	–	–	0.02266	0.02184
10	–	0.00971	0.01000	–	–	0.05414	0.05169
11	–	–	–	0.00356	0.01559	0.02914	0.02737
12	–	–	–	0.01035	0.01242	0.03043	0.02549
13	0.01461	–	–	0.01488	0.00634	–	–
14	0.02306	0.02783	0.02395	0.02394	0.03032	–	–
15	0.03051	0.03107	0.02460	–	–	0.03947	0.04865
16	0.02105	–	–	0.02013	0.02711	0.03912	0.04064
17	–	0.01681	0.01744	0.01844	0.02605	0.03561	0.03477
18	0.03950	0.04951	0.03721	0.03429	0.05172	0.04532	0.04040
19	0.03265	0.05501	0.02227	0.02717	0.04683	0.04111	0.03493
20	0.03288	0.03689	0.03355	0.01423	0.05846	0.04597	0.02932
21	0.03791	0.04336	0.03681	0.03332	0.04716	0.06345	0.02946

each of these Rietveld analyses. Examination of the results in Table 4 immediately indicates that the Rietveld method is a very accurate tool for the determination of the lattice parameters of the polytypes in SiC ceramics because the mean and maximum relative errors of these Rietveld analyses are as low as 0.02549% and 0.06345% (this latter for the most unfavourable case of coexistence of 4 polytypes), respectively. Nevertheless, one also notes in Table 4 that the accuracy of the Rietveld method decreases with increasing number of polytypes in the SiC ceramic because the mean relative error of the Rietveld analyses for the cases with two (simulations 1–13), three (simulations 14–17), and four (simulations 18–21) polytypes are 0.01544%, 0.02860%, and 0.03931%, respectively. This trend can be satisfactorily explained by considering simply that the severity of the peak overlap phenomenon in the XRD patterns of the multiphase materials increases with increasing number of phases, and that, as can be seen in Fig. 1, the direct effect of the peak overlap is to shift the apparent position of the diffraction peaks from the Bragg positions as well as to broaden them asymmetrically. This by itself reduces the accuracy in the determination of the positions of the individual Bragg reflections, with the corresponding loss of accuracy in the measurement of lattice parameters. In the particular case of the SiC ceramics the scenario is further aggravated because the peak overlap phenomenon is so severe that the individual Bragg reflections actually form groups of reflections, which in turn can also themselves overlap, thus making it even more difficult to evaluate accurately the lattice parameters of the polytypes, with the greater the number of polytypes the greater the difficulty. These effects are illustrated by the example of Fig. 2, which compares the XRD patterns for the combinations of polytypes 4H–15R and 3C–4H–6H–15R.

Another feature of interest in Table 4 is that the accuracy of the Rietveld method is conditioned by the specific polytypes present in the SiC ceramic, not only by their number. This is made more evident in Table 5, which gives the mean relative error of the Rietveld analyses for the different possible combinations of two and three polytypes. Consider in first instance the systems with two polytypes. It can be observed in Table 5 that the maximum relative error in the measurement of the lattice parameter of the 3C polytype occurs in the 3C–6H combination, followed by the 3C–4H combination, and lastly by the 3C–15R combination. The corresponding sequences of maximum relative errors for the polytypes 4H, 6H, and 15R are 4H–3C > 4H–15R > 4H–6H, 6H–3C > 6H–4H > 6H–15R, and 15R–4H > 15R–6H > 15R–3C, respectively. To explain these trends, we calculated for each simulated polytype combination the number of Bragg reflections without overlap of each individual polytype between 29° and 101° 2θ as well as the sum for all the polytypes. The results are also given in Table 5. For this calculation, two Bragg reflections were taken as being overlapped when their maxima differed by less than 0.4° 2θ. This overlap condition was chosen on the base of numerous

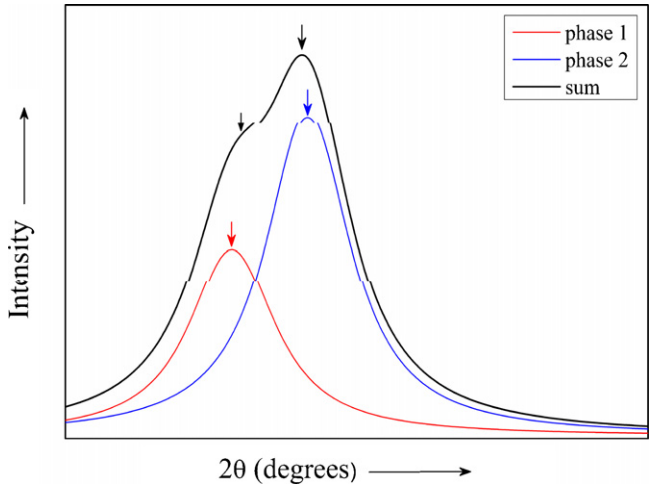

Fig. 1. Example of the peak shifting and peak asymmetry in the XRD patterns of multiphase materials induced by the peak overlap (only two peaks in this case).

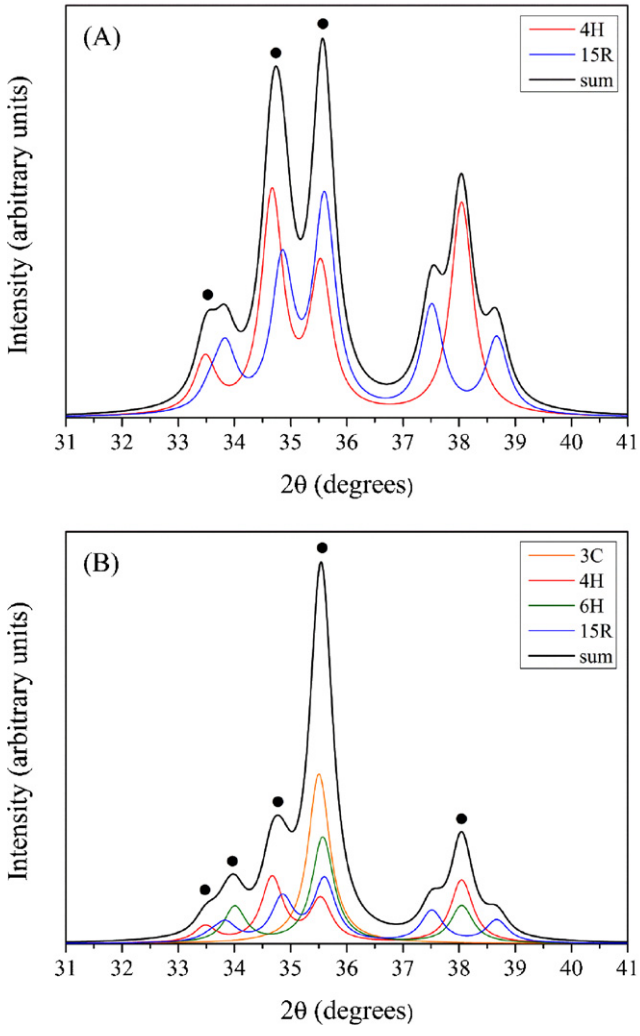

Fig. 2. XRD patterns (region 31–41° 2θ) of the SiC ceramics composed of the polytypes (A) 4H and 15R, and (B) 3C, 4H, 6H, and 15R. The symbol ● denotes the formation of a peak group. In A: the first group is 100–4H + 101–15R; the second group is 101–4H + 104–15R; the third group is 004–4H + 015–15R. In B: the first group is 100–4H + 100–6H + 101–15R; the second group is 101–6H + 012–15R; the third group is 101–4H + 104–15R; the fourth group is 111–3C + 004–4H + 102–6H + 015–15R; 102–4H + 103–6H; the fifth group is 102–4H + 103–6H.

Table 5
Number of Bragg reflections free of overlap and mean relative error in the measurement of the lattice parameter per polytype for the different possible combinations of two and three SiC polytypes.

Polytype system	Non-overlapped Bragg reflections per each polytype	Total non-overlapped Bragg reflections	Mean error of the Rietveld analyses per each polytype (%)
3C–4H	2–17	19	0.009705–0.013815
3C–6H	0–12	12	0.018040–0.017257
3C–15R	0–30	30	0.002740–0.004428
4H–6H	14–11	25	0.010475–0.011545
4H–15R	8–16	24	0.011615–0.037583
6H–15R	9–17	26	0.010489–0.028107
3C–4H–6H	0–14–11	25	0.02306–0.02589–0.02713
3C–4H–15R	0–8–16	24	0.03051–0.02783–0.04406
3C–6H–15R	0–9–17	26	0.02105–0.02362–0.03988
4H–6H–15R	8–9–16	33	0.01712–0.02224–0.03519

observations of peak overlap for SiC polytypes with crystallite sizes of 20 nm, and will be used only within the context of the present study because it must be expected to change if the crystallite size changes. Besides, for the calculation only the Bragg reflections whose intensity was greater than 5% of the most intense Bragg reflection were taken into account, since weaker Bragg reflections may mingle with the background and noise. As can be observed in Table 5, there exists a clear correlation between the errors of the Rietveld analyses and the total number of Bragg reflections free of overlap, with the errors decreasing as the total number of non-overlapped Bragg reflections increases. This latter is due to the use during the Rietveld refinements of a broader set of accurate interplanar spacings for the calculation of the lattice parameters, and to the fact that the lattice parameters of the different polytypes present are not refined independently because the Rietveld method pursues the best agreement between the whole observed and calculated XRD patterns [19]. The same observations and conclusions are also valid when one examines the three-polytype combinations, as can also be deduced from Table 5. The accuracy of the Rietveld analyses, however, does not seem to be affected by the exact concentrations of the different polytypes. This is consistent with the fact that the Rietveld method not only fits the scale factor of each phase present, but also weighs the individual intensities over the entire XRD pattern during the fitting procedure [19].

Influence of the polytype crystallite size

Table 6 gives the lattice parameters of the SiC polytypes calculated by the Rietveld method for the second series of 21 standard XRD patterns, and Table 7 lists the relative error of

Table 6
Lattice parameters of the SiC polytypes determined by the Rietveld method for the second series of 21 simulated standard XRD patterns, designed to investigate crystallite-size effects in the determination of lattice parameters.

No.	Lattice parameters determined from the Rietveld analysis (Å)		
	a_{3C}	a_{6H}	c_{6H}
1	4.37972(12)	3.0916(11)	15.14124(40)
2	4.37963(9)	3.09158(9)	15.14095(36)
3	4.37959(8)	3.09156(8)	15.14080(26)
4	4.37949(7)	3.09151(7)	15.14046(19)
5	4.37945(7)	3.09145(5)	15.14033(15)
6	4.37937(5)	3.09138(3)	15.14011(13)
7	4.37935(3)	3.09135(2)	15.14010(10)
8	4.37962(10)	3.09158(15)	15.14091(39)
9	4.37959(9)	3.09153(10)	15.14081(34)
10	4.37957(7)	3.09150(8)	15.14074(28)
11	4.37954(6)	3.09147(6)	15.14067(24)
12	4.37952(4)	3.09145(6)	15.14058(23)
13	4.37947(4)	3.09143(5)	15.14042(20)
14	4.37944(2)	3.09142(3)	15.14032(15)
15	4.37847(30)	3.09192(33)	15.13738(57)
16	4.38009(16)	3.09189(14)	15.14211(45)
17	4.37969(12)	3.09166(10)	15.14116(34)
18	4.37954(8)	3.09150(7)	15.14062(25)
19	4.37943(6)	3.09122(5)	15.13921(15)
20	4.37936(2)	3.09133(2)	15.14011(5)
21	4.37927(2)	3.09131(2)	15.13950(5)

Table 7
Absolute value of the relative difference between the lattice parameters of the SiC polytypes calculated by the Rietveld method and those used as inputs in the simulations of the second series of 21 standard XRD patterns, designed to investigate crystallite-size effects in the determination of lattice parameters.

No.	Error of the Rietveld analysis (%)		
	a_{3C}	a_{6H}	c_{6H}
1	0.00959	0.00970	0.00951
2	0.00754	0.00906	0.00760
3	0.00662	0.00841	0.00661
4	0.00434	0.00679	0.00436
5	0.00343	0.00485	0.00350
6	0.00160	0.00259	0.00205
7	0.00114	0.00162	0.00198
8	0.00722	0.00906	0.00733
9	0.00656	0.00744	0.00667
10	0.00623	0.00647	0.00621
11	0.00558	0.00550	0.00575
12	0.00492	0.00485	0.00515
13	0.00394	0.00421	0.00409
14	0.00328	0.00388	0.00343
15	0.01901	0.01998	0.01601
16	0.01808	0.01951	0.01532
17	0.00891	0.01165	0.00898
18	0.00548	0.00647	0.00542
19	0.00297	0.00259	0.00390
20	0.00137	0.00097	0.00205
21	0.00069	0.00032	0.00198

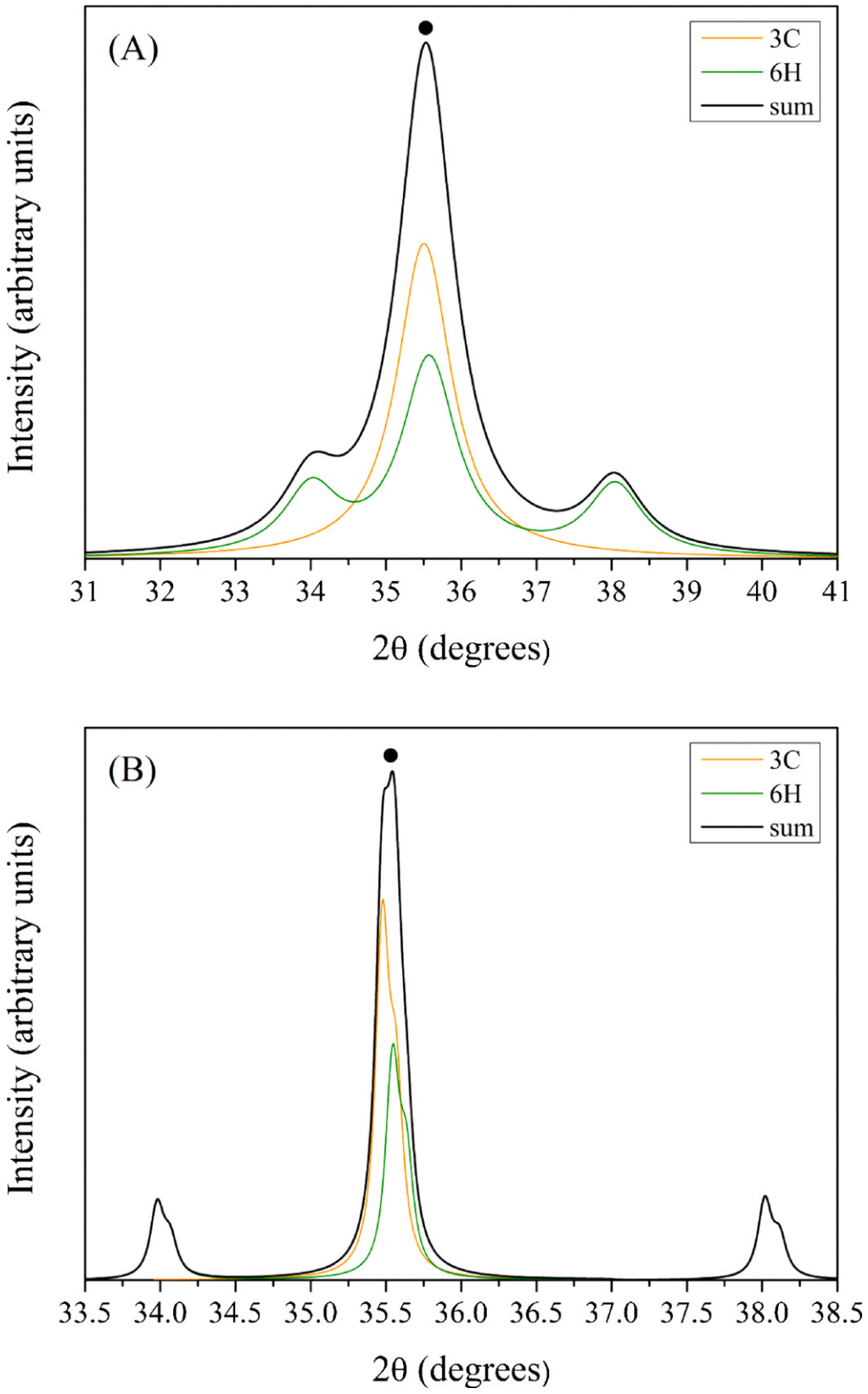

Fig. 3. XRD patterns (region 31–41° 2θ) of the SiC ceramics composed of the polytypes 3C and 6H both with crystallite sizes of (A) 5 nm, and (B) 0.5 μm. The symbol ● denotes the formation of a peak group (111–3C + 102–6H). Note in (B) the clear splitting of the Cu Kα_1 and Cu Kα_2 doublet.

each of these Rietveld analyses. Again, one notes in Table 7 that the accuracy of the Rietveld refinements is extremely high, with the maximum error in the measurement of the lattice parameters being as low as 0.01998% (this value corresponds to the most unfavourable case of 5 nm crystallite size for both the 3C and 6H polytypes). Examination of the results in Table 7 also indicates that the accuracy of the Rietveld analyses depends on the crystallite size of the polytypes. For example, consider the first 7 cases in which the crystallite size of the 6H polytype is kept constant at 50 nm and that of the 3C polytype is varied in the 5–500 nm interval. It is clear that the errors of the Rietveld analyses initially decrease rapidly with increasing crystallite size from 5 nm up to ~100 nm, then more slowly with the increase from 100 to ~200 nm, and finally do not fall much once the crystallite size is above 200 nm. This type of trend is also observed when the crystallite size of the 3C polytype is kept constant at 50 nm and that of the 6H polytype is varied in the 5–500 nm interval, and when the crystallite sizes of both polytypes are varied simultaneously. Comparing the results for the three sub-series themselves, one also notes that the simultaneous variation of the crystallite size of the two polytypes (i.e., the third sub-series) has greater impact on the accuracy of the Rietveld method than the variation of only the crystallite size of one of the two polytypes (i.e., the first and second sub-series), in which case the errors are more conditioned by the variation of the crystallite size of the 3C polytype (i.e., the first sub-series) than by the variation of the crystallite size of the 6H polytype (i.e., the second sub-series).

The decreasing trend of the errors of the Rietveld analyses with increasing crystallite size of the polytypes can be explained well by alluding to the line-broadening theory of X-ray diffraction. This theory posits an inverse relationship between the width (w) of the XRD peaks and the crystallite size (D) [16,17,24,25]. With this $w \propto D^{-1}$ dependence, the XRD peaks broaden with decreasing crystallite size, and this peak broadening has in turn a doubly detrimental effect on the accuracy of the Rietveld method in determining lattice parameters. Firstly, the Bragg reflections become blunter, causing loss of definition in the location of the peak maxima. And secondly, the Bragg reflections have tails extending over a wider 2θ range, so that the severity of the undesirable peak overlaps increases, with the attendant aggravation of the phenomena of the peaks shifting from the Bragg positions and of the peak asymmetry. These effects are illustrated in the example of Fig. 3, which compares the XRD patterns for the combination of polytypes 3C–6H with crystallite sizes of 5 nm or 0.5 μm.

The former explanation also accounts for the observation that the accuracy of the Rietveld-calculated lattice parameters levels off at about 200 nm. Above a certain crystallite size, in particular above the ultrafine range, crystallite size effects in the peak width become negligible, and the peak broadening is entirely due to instrumental broadening. In this scenario, increasing the crystallite size no longer broadens the XRD peaks, and therefore no longer conditions the measurement of the lattice parameters either. The blunting and broadening effects also explain the greater dependence of the errors with the simultaneous variation of the crystallite size of the two polytypes because of the larger differences between extreme cases. Thus, in one extreme the nanostructuring is far more severe (i.e., 5 nm crystallite size for both polytypes, instead of 5 nm for one and 50 nm for the other) and in the other extreme the microstructure consists entirely of large crystallites (i.e., 0.5 μm crystallite size for both polytypes, instead of 50 nm for one and 0.5 μm for the other) and, consequently, the XRD peaks change from being much blunter and broader to being much sharper and narrower. This greater change in the blunting and broadening explains the greater variation from a larger value down to a lower value observed in the errors of the Rietveld analyses. Finally, the fact that the accuracy of the Rietveld-calculated lattice parameters depends more on the variation of the crystallite size of the 3C polytype than on that of the 6H polytype is simply because, when the two co-exist, the 3C polytype has no overlap-free Bragg reflections whereas the 6H polytype does have some well-resolved Bragg reflections (see Table 5) so that their broadening or sharpening has less impact on the measurement of the lattice parameters.

Conclusions

We have investigated the dependence of the accuracy of the measurement of the lattice parameters of polytypes in multiphase SiC ceramics by the Rietveld method on the polytype composition and polytype crystallite size. The results allow the following conclusions to be drawn:

1. The Rietveld method is remarkably accurate, and provides a very appropriate framework for the determination of the lattice parameters of polytypes in SiC ceramics via conventional XRD. It may therefore help to better characterize SiC ceramics.
2. The accuracy of the Rietveld analyses decreases with increasing number of polytypes, and for a given number of polytypes it is also conditioned by the specific polytypes present. These findings reflect that the error of the Rietveld refinements is affected by the severity of the peak overlap phenomenon in the XRD patterns. The accuracy of the Rietveld analyses does not show, however, any clear correlation with the exact concentrations of the different polytypes, which is due to the use of scale factors for the different phases and to the weighting of the intensities during the implementation of the Rietveld refinements.
3. The accuracy of the Rietveld analyses decreases with decreasing crystallite size of the polytypes. This is because the peak broadening caused by the reduction in the crystallite size induces both a loss of definition in the location of the peak maxima and greater severity of the peak overlaps, both of which factors are detrimental to the measurement of lattice parameters.

Acknowledgements

This work was supported by the Ministerio de Ciencia y Tecnología (Government of Spain) and FEDER funds under Grant No. MAT 2010-16848.

References

[1] F. Rodríguez-Rojas, A.L. Ortiz, F. Guiberteau, M. Nygren, Oxidation behaviour of pressureless liquid-phase-sintered α-SiC with additions of $5Al_2O_3 + 3RE_2O_3$ (RE = La, Nd, Y, Er, Tm, or Yb), J. Eur. Ceram. Soc. 30 (15) (2010) 3209–3217.

[2] F. Rodríguez-Rojas, A.L. Ortiz, F. Guiberteau, M. Nygren, Anomalous oxidation behaviour of pressureless liquid-phase-sintered SiC, J. Eur. Ceram. Soc. 31 (13) (2011) 2393–2400.

[3] H. Ye, V.V. Pujar, N.P. Padture, Coarsening in liquid-phase-sintered α-SiC, Acta Mater. 47 (2) (1999) 481–487.

[4] H. Xu, T. Bhatia, S.A. Deshpande, N.P. Padture, A.L. Ortiz, F.L. Cumbrera, Microstructural evolution in liquid-phase-sintered SiC. I. Effect of starting powder, J. Am. Ceram. Soc. 84 (7) (2001) 1578–1584.

[5] S.A. Deshpande, T. Bhatia, H. Xu, N.P. Padture, A.L. Ortiz, F.L. Cumbrera, Microstructural evolution in liquid-phase-sintered SiC. II. Effects of planar defects densities and seeds in the starting powder, J. Am. Ceram. Soc. 84 (7) (2001) 1585–1590.

[6] A.L. Ortiz, T. Bhatia, N.P. Padture, G. Pezzotti, Microstructural evolution in liquid-phase-sintered SiC. III. Effect of atmosphere, J. Am. Ceram. Soc. 85 (7) (2002) 1835–1840.

[7] L.S. Sigl, H.-J. Kleebe, Core/rim structure of liquid-phase-sintered silicon carbide, J. Am. Ceram. Soc. 76 (3) (1993) 773–776.

[8] N.W. Jepps, T.F. Page, Polytypic transformation in silicon carbide, in: P. Krishna (Ed.), Crystal Growth and Characterization of Polytype Structures, vol. 7, Pergamon Press, Oxford, UK, 1983 , pp. 259–307.

[9] N.P. Padture, *In situ*-toughened silicon carbide, J. Am. Ceram. Soc. 77 (2) (1994) 519–523.

[10] O. Borrero-López, A.L. Ortiz, F. Guiberteau, N.P. Padture, Sliding-wear-resistant liquid-phase-sintered SiC processed using α-SiC starting powders, J. Am. Ceram. Soc. 90 (2) (2007) 541–545.

[11] H. Tanaka, N. Hirosaki, T. Nishimura, D.-W. Shin, S.-S. Park, None-quiaxial grain growth and polytype transformation of sintered α-silicon carbide and β-silicon carbide, J. Am. Ceram. Soc. 86 (12) (2003) 2222–2224.

[12] O. Borrero-López, A. Pajares, A.L. Ortiz, F. Guiberteau, Hardness degradation in liquid-phase-sintered SiC with prolonged sintering, J. Eur. Ceram. Soc. 27 (11) (2007) 3359–3364.

[13] T.E. Mitchell, A.H. Heuer, Solution hardening by aliovalent cations in ionic crystals, Mater. Sci. Eng. 28 (81) (1977) 81–97.

[14] O. Borrero-López, A.L. Ortiz, F. Guiberteau, N.P. Padture, Effect of microstructure on sliding-wear properties of liquid-phase-sintered α-SiC, J. Am. Ceram. Soc. 88 (8) (2005) 2159–2163.

[15] J. Sánchez-González, A.L. Ortiz, F. Guiberteau, C. Pascual-Centenera, Complex impedance spectroscopy study of a liquid-phase-sintered α-SiC, J. Eur. Ceram. Soc. 27 (13–15) (2007) 3941–3945.

[16] H.P. Klug, L.E. Alexander, X-ray Diffraction Procedures for Polycrystalline and Amorphous Materials, Wiley, New York, 1974.

[17] B.D. Cullity, Elements of X-ray Diffraction, Addison-Wesley, Boston, MA, 1978.

[18] H.M. Rietveld, A profile refinement method for nuclear and magnetic structures, J. Appl. Crystallogr. 2 (2) (1969) 65–71.

[19] R.A. Young, The Rietveld Method, Oxford University Press, Oxford, UK, 1993.

[20] A. Hernández-Jiménez, A.L. Ortiz, F. Sánchez-Bajo, F. Guiberteau, F.L. Cumbrera, Determination of lattice parameters of polytypes in liquid-phase-sintered SiC using the Rietveld method, J. Am. Ceram. Soc. 87 (5) (2004) 943–949.

[21] A. Lara, A.L. Ortiz, A. Muñoz, A. Domínguez-Rodríguez, Densification of additive-free polycrystalline β-SiC by spark-plasma sintering, Ceram. Int. 38 (1) (2012) 45–53.

[22] R.D. Shannon, Revised effective ionic radii and systematic studies of interatomic distances in halides and chalcogenides, Acta Crystallogr. A32 (5) (1976) 751–767.

[23] A.L. Ortiz, F.L. Cumbrera, F. Sánchez-Bajo, F. Guiberteau, H. Xu, N.P. Padture, Quantitative phase-composition analysis of liquid-phase-sintered silicon carbide using the Rietveld method, J. Am. Ceram. Soc. 83 (9) (2000) 2282–2286.

[24] R.L. Snyder, J. Fiala, H.J. Bunge, Defect and Microstructure Analysis by Diffraction, Oxford University Press, Oxford, UK, 1999.

[25] E.J. Mittemeijer, P. Scardi, Diffraction Analysis of the Microstructure of Materials, Springer-Verlag, Berlin, Germany, 2004.